Applied Surface Science 254 (2008) 5827–5830

Contents lists available at ScienceDirect

Applied Surface Science

journal homepage: www.elsevier.com/locate/apsusc

A DFT study of H adsorption on Pt(111) and Pt–Ru(111) surfaces

Carolina Pistonesi, Estela Pronsato, Alfredo Juan *

Departamento de Física, Universidad Nacional del Sur, Avda. Alem 1253, 8000 Bahía Blanca, Argentina

ARTICLE INFO

Article history:
Received 11 July 2007
Accepted 16 March 2008
Available online 4 April 2008

PACS:
71.15.Mb
73.20.At
81.05.Bx

Keywords:
Pt–Ru
Alloy
Hydrogen
DFT

ABSTRACT

In this work a comparative analysis between different Pt–Ru(111) surface models and pure Pt(111) surface is presented. Some aspects of the electronic structure of the surfaces and hydrogen adsorption are analysed based on density functional theory calculations. The hydrogen adsorption energy is significantly reduced when Ru is present on the surface. The substitution of Pt atoms by Ru atoms reinforce the Pt–H bond while the metal–metal bond is strongly modified, making the system less stable.

1. Introduction

Platinum is a well-known anodic material when pure hydrogen is used in fuel cells. The H_2 used as a fuel is usually produced from natural gas or from methanol. CO is a by-product of such processes and as little as 20 ppm of CO in the H_2 stream severely poisons a pure Pt catalyst surface [1]. This problem can be alleviated by alloying Pt with other metals like Ru, Sn or Mo, which produces anodes much more tolerant than pure Pt catalysts [2–4].

The composition of Pt–Ru alloys plays an important role in the methanol oxidation processes. At compositions up to 60 at.% Ru, the alloy is formed as a substitutional solid solution where Pt atoms from the fcc structure are replaced by Ru atoms [5]. Electrochemical measurements and X-ray diffraction techniques have determined that the catalytic activity for methanol electro-oxidation exhibits a maximum at about 50 at.% Ru [6]. Other studies suggest optimal Pt–Ru compositions with lower Ru surface contents in the range of 10–40 at.% Ru [7–9]. However, it has been pointed out that the optimal Pt–Ru composition for methanol oxidation depends on the preparation of Pt–Ru catalyst [10].

In this work a comparative analysis between different Pt–Ru(111) surface models and a pure Pt(111) surface is presented. Some aspects of the electronic structure of the surfaces and hydrogen adsorption are studied using density functional theory (DFT) calculations.

2. Computational method

The generalized gradient approximation (GGA) to the DFT is used to study Pt(111) and Pt–Ru(111) surface alloy and its interaction with hydrogen. The calculations were carried out using the ADF2004.01 package [11–13].

For the gradient correction the Becke [14] approximation for the exchange energy functional and the LYP [15] approximation for the correlation functional were employed. In order to increase the computational efficiency, the internal atomic layers are kept frozen for every atom, except hydrogen, since the internal electrons do not contribute significantly to the bonding. A triple-zeta basis set of Slater type orbitals was used for valence electrons which include an additional set of functions for each element, playing the role of polarization functions. The frozen core orbitals include up to 4d and 3d orbitals for Pt and Ru atoms, respectively on the central part of the cluster that represent the metallic surface. For the other surrounding atoms, the frozen core orbitals include up to 4f and 4p orbitals for Pt and Ru atoms, respectively.

To understand the interactions between different atoms we used the concepts of DOS (density of states) and COOP (crystal orbital overlap population) curves. The DOS curve is a plot of the

* Corresponding author. Tel.: +54 291 4595143; fax: +54 291 4595142.
E-mail address: cajuan@criba.edu.ar (A. Juan).

0169-4332/$ – see front matter © 2008 Elsevier B.V. All rights reserved.
doi:10.1016/j.apsusc.2008.03.167

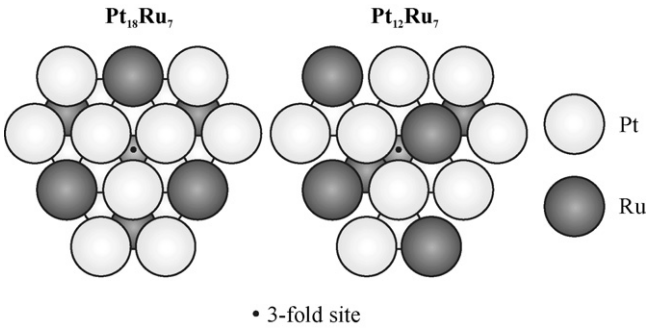

Fig. 1. Geometry of $Pt_{18}Ru_7$ and $Pt_{12}Ru_7$ clusters. A threefold site is determined at the canter of the surface of the cluster.

number of orbitals per unit energy. The COOP curve is a plot of the overlap population (OP) weighted DOS versus energy. The integration of the COOP curve up to the Fermi level (E_F) gives the total overlap population of a specified bond and it is a measure of the bond strength.

3. The cluster model of the metal surface

A cluster was used to represent the Pt(111) surface. It is composed of 25 Pt atoms (Pt_{25}) distributed in three (111) layers of 12, 6 and 7 atoms each, sequentially stacked from the surface. Above the centre of the surface layer there is a threefold tetrahedral (or hollow) adsorption site. The distance between first neighbour Pt atoms is 2.77 Å and the distance between (111) layers is 2.26 Å.

In order to represent the Pt–Ru alloy surface, some atoms of the Pt_{25} cluster were substituted by Ru atoms. Following this procedure two clusters were built, each one containing three (111) layers with a threefold site in the centre of the surface. On the $Pt_{18}Ru_7$ cluster there are Ru atoms second neighbours to the central threefold site while on $Pt_{12}Ru_7$ there is one Ru atom first neighbour to that site, as shown in Fig. 1. $Pt_{12}Ru_7$ was built smaller in order to diminish convergence problems on calculations, because this cluster is less symmetric than the $Pt_{18}Ru_7$ cluster.

Both experimental and theoretical results indicate the preference of H atoms to threefold sites on pure platinum surfaces [16–18]. The same fcc site was also the most stable found with DFT calculations on a Pt overlayer on Ru(0001) and Pt_3Sn(111) alloy [19]. So hydrogen adsorption on a threefold site is analysed in all surfaces.

Table 1
d bandwidth, charges and atomic orbital populations for surface Pt and Ru, 2nd layer Pt atoms and H atom

System	d bandwidth (eV)	Atom	Charge	Orbital occupation		
				s	p	d
Pt_{25}	5.44	Pt	−0.1568	2.5632	6.4218	9.1714
		Pt[a]	0.0808	2.4188	6.4933	9.0071
H/Pt_{25}	5.27	Pt	0.1627	2.4176	6.2427	9.1766
		Pt[a]	0.0785	2.3893	6.4661	9.0660
		H	−0.3861	1.2361	0.1500	0.0000
$Pt_{18}Ru_7$	6.19	Ru	0.2471	2.5561	6.2175	6.9793
		Pt	−0.2084	2.5988	6.4896	9.1194
		Pt[a]	0.3657	2.1960	6.4485	8.9897
$H/Pt_{18}Ru_7$	5.59	Ru	0.1760	2.5535	6.2966	6.9739
		Pt	0.0504	2.5077	6.3197	9.1219
		Pt[a]	0.3299	2.1953	6.4538	9.0209
		H	−0.3108	1.1720	0.1388	0.0000
$Pt_{12}Ru_7$	6.28	Pt	0.0640	2.4115	6.4111	9.1129
		Ru	0.1731	2.5125	6.4133	6.9011
		Pt[a]	0.1384	2.4334	6.3690	9.0591
$H/Pt_{12}Ru_7$	5.74	Pt	0.2858	2.3372	6.2712	9.1054
		Ru	0.3126	2.3574	6.4540	6.8760
		Pt[a]	0.0913	2.4393	6.3780	9.0914
		H	−0.3062	1.2201	0.0861	0.0000

[a] Second layer Pt atom close to the surface threefold site.

4. Results and discussion

Let us discuss first some aspects of the electronic structure of the clean surfaces, after that, the hydrogen adsorption will be analysed. Table 1 summarizes the electronic orbital populations and charges for different atoms on the central part of each cluster.

From the results corresponding to Pt_{25} cluster it is observed that surface atoms have higher electron density than those in the second layer. Surface Pt–Pt bonds are weaker than Pt bonds between the first and the second layer, as indicated by the overlap population values in Table 2.

Fig. 2a (filled line) shows the DOS curve for the Pt_{25} cluster. The energy region between −9.0 and −3.6 eV corresponds to the d band mixed with s states on its lower energy part.

As mentioned before, the bonding study was performed analysing the COOP curves. For a surface Pt–Pt bond, the COOP curve in Fig. 3a shows bonding interactions at low energy values and antibonding peaks for higher energies below the Fermi level

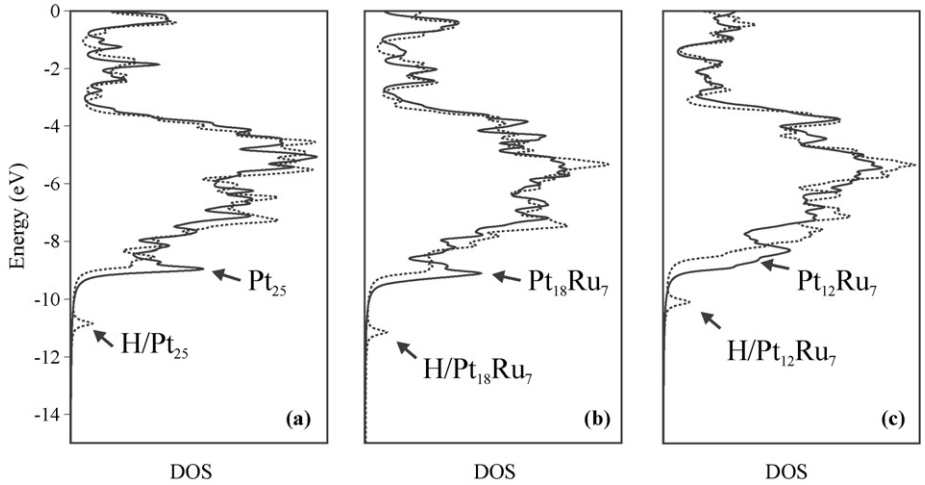

Fig. 2. Density of states (DOS) for Pt_{25} (filled line) and H/Pt_{25} (dotted line) (a); DOS for $Pt_{18}Ru_7$ (filled line) and $H/Pt_{18}Ru_7$ (dotted line) (b); DOS for $Pt_{12}Ru_7$ (filled line) and $H/Pt_{12}Ru_7$ (dotted line) (c).

Table 2
Overlap population (OP) values

System	Pt–Pt		Pt–H	Pt–Ru	H–Ru
	Surface	1st–2nd layer			
Pt_{25}	0.0104	0.0273	–	–	–
H/Pt_{25}	0.0089	0.0122	0.0611	–	–
$Pt_{18}Ru_7$	0.0209	0.0138	–	0.0210	–
$H/Pt_{18}Ru_7$	0.0151	0.0006	0.0831	0.0726	–
$Pt_{12}Ru_7$	0.0194	0.0065	–	0.0137	–
$H/Pt_{12}Ru_7$	0.0007	0.0003	0.1335	0.0179	0.0712

Two types of Pt–Pt bonds are considered: both Pt atoms on the surface, and one Pt atom on the surface and the other on the 2nd layer. In all cases the closest bonds to the surface threefold site are considered (not always first neighbours to it).

(E_F). A similar bonding scheme was obtained using Extended Hückel and DFT formalisms [18].

Adsorption energies and H–Pt optimized distances are shown in Table 3. These values are very similar to those obtained previously with semiempirical calculations [20], although experimental H–Pt distances are slightly higher (1.8–1.9 Å) [16]. When H is adsorbed on the platinum surface, the s and p orbital populations of surface Pt atom decrease 6% and 3%, respectively, resulting a reduction on surface Pt charge of $0.319e^-$. Pt atoms from the second layer suffer only a small change on its atomic orbital occupation. H atom gains a negative charge of $-0.386e^-$, so there is a transference of electron density from the platinum surface atoms to the adsorbed hydrogen. Similar behaviour has been observed in similar metal–hydrogen systems [18–20].

The DOS curve after H adsorption on pure platinum surface (Fig. 2a, dotted line), shows an additional peak at −10.8 eV composed mainly by H states and Pt d states with a small contribution of Pt s states. The DOS curve also shows a narrower d band when compared with a pure platinum d band (also see d

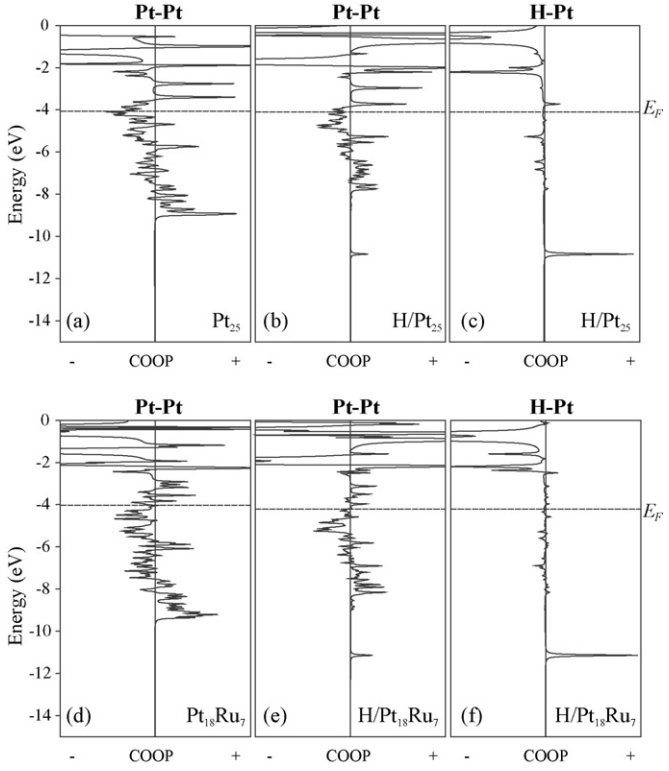

Fig. 3. COOP curves for surface bonds: Pt–Pt on Pt_{25} (a) and on H/Pt_{25} (b); H–Pt on H/Pt_{25} (c); Pt–Pt on $Pt_{18}Ru_7$ (d) and on $H/Pt_{18}Ru_7$ (e); H–Pt on $H/Pt_{18}Ru_7$ (f). The COOP range is three times bigger on Pt–H (c and f).

Table 3
Adsorption energies (E_{ads}) and distances from adsorbed H to first neighbour surface Pt atom (d_{H-Pt})

System	H/Pt_{25}	$H/Pt_{18}Ru_7$	$H/Pt_{12}Ru_7$
E_{ads} (eV)	−1.90	−1.22	−1.17
d_{H-Pt} (Å)	1.74	1.75	1.83

bandwidth in Table 1). The DOS intensity peak is lower for the energy region from −10 to −8 eV (region of Pt–Pt bonding peaks) and is higher in the region from −8 to −4 eV (zone of Pt–Pt antibonding peaks) than the corresponding DOS for pure platinum. As a result there is a reduction on the Pt–Pt OP value when H is adsorbed (see Table 2 and the corresponding COOP curve in Fig. 3b). The COOP curve for the H–Pt interaction (Fig. 3c) shows that the peak at −10.8 eV corresponds to a bonding interaction. We can conclude then, that hydrogen bonds to the surface at expenses of weakening Pt–Pt bonds close to it.

In the $Pt_{18}Ru_7$ cluster the surface Pt atoms show higher electron density than surface Ru atoms (see Table 1). There is also an important decrease on the charge of second layer Pt atoms. The DOS curve in Fig. 2b (filled line) shows a broadening in the d band (see also Table 1). This broadening of the d band has also been found under DFT calculations on Pt(111) slabs containing subsurface 3d metals [21].

The COOP curve for Pt–Pt surface bond (Fig. 3d) reveals a wider energy window for bonding peaks on the low energy part and also smaller antibonding peaks at high energy levels (below E_F). As a result the net OP value for Pt–Pt bond is higher than in the case of pure platinum surface. In the alloy, the surface Pt–Pt bonds close to Ru atoms are stronger than Pt bonds between the surface and the second layer (see Table 2).

The H adsorption energy is 35% lower in the alloy surface, when compared with a pure Pt surface. The electronic charge of surface Pt atom is reduced by $0.259e^-$ due to a decrease on s and p orbital occupation of 3.5% and 2.5%, respectively, when compared with the clean alloy surface. The Ru atom (second neighbour to the adsorption site) has a small increase of $0.07e^-$ on its charge due to an increase on p orbital occupation of 1.3%. The electron transference towards H atom is $-0.311e^-$ (smaller than on Pt_{25}). There is again a reduction on Pt–Pt OP value when H is adsorbed (see Table 2 and corresponding COOP curve in Fig. 3e). The peak at −11.15 eV corresponds to a H–Pt bonding interaction (see Fig. 3f).

The DOS curve in Fig. 2b (dotted line) shows a peak at −11.15 eV (similar to the case of the adsorption on the pure metal surface), in which there is no participation of Ru states. The d bandwidth suffers an important reduction when H is adsorbed (see Table 1).

Although our calculations show an increase on the OP value for the H–Pt bond, the OP value for the Pt–Pt bonds decrease more than in the pure platinum surface. When analysing the Pt–Ru interaction we can see that Pt–Ru bond reinforce after H adsorption (see Table 2 and Fig. 4a and b). Note that there is no bonding or antibonding contribution at −11.15 eV due to the fact that Ru atom is second neighbour to the adsorption site.

Similar results are obtained for the $Pt_{12}Ru_7$ alloy model. In this cluster one Ru atom is first neighbour to the adsorption site, and the adsorption energy and charge transference towards the H atom ($-0.306e^-$) are lower than in the previous case. The proximity to Ru is responsible of these changes. DOS curves (Fig. 2c) are similar to those for the $Pt_{18}Ru_7$ alloy (also COOP curves, which are not included in Fig. 3). For this alloy model the presence of H produces a higher weakening on Pt–Pt bonds (see Table 2). When compare all the results we can see that the percentage of Pt–Pt bond weakening close to H increase with the proximity to Ru: 15%(pure Pt), 28%(Ru 2nd neighbor) and 96% (Ru 1st neighbor).

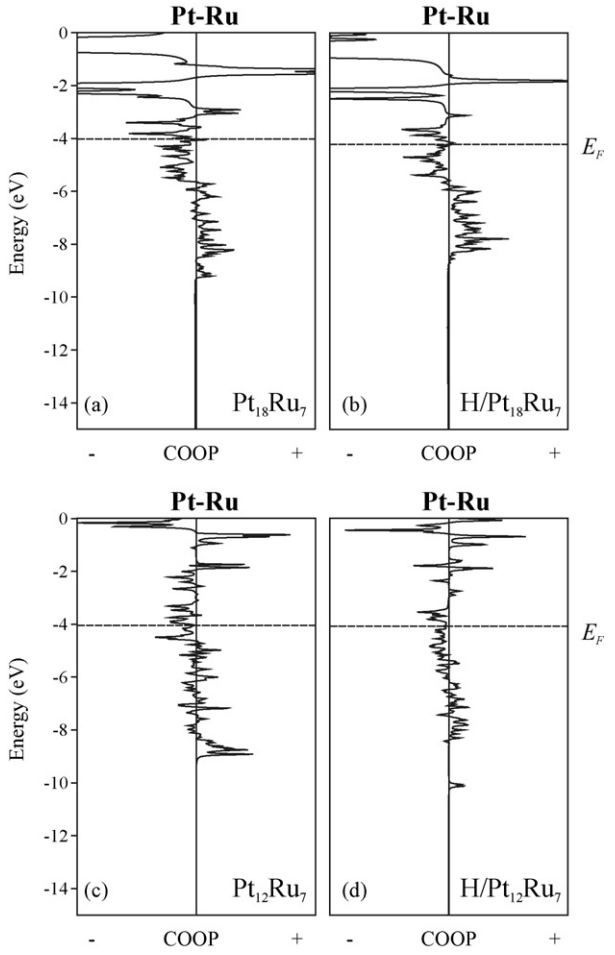

Fig. 4. COOP curves for Pt–Ru interaction on $Pt_{18}Ru_7$ (a), $H/Pt_{18}Ru_7$ (b), $Pt_{12}Ru_7$ (c) and $H/Pt_{12}Ru_7$ (d).

For the $Pt_{12}Ru_7$ cluster there is only a small reinforce of Pt–Ru bond when H is adsorbed (see Table 2 and Fig. 4c and d). This bond is first neighbor to the adsorption site and although there is a bonding contribution due to the H peak, more antibonding contributions are present, due to the proximity to the H atom.

5. Conclusions

In this work the H adsorption on Pt(111) and on two Pt–Ru(111) alloy surfaces were studied using density functional theory and clusters to represent the alloy surfaces.

Ru atoms induce changes on the electronic structure of Pt producing a broadening of the d bandwidth. The hydrogen adsorption energy is significantly reduced when Ru is present. According to our calculations, although locally there is a reinforce of H–Pt bond, the weakening of the Pt–Pt bonds close to the adsorption site is very strong in the presence of Ru, producing a less stable system.

Acknowledgements

The authors thank Departamento de Física UNS, SGECyT, CONICET, CIC Pcia. Bs. As. and Guggenheim Foundation for their financial support. C. Pistonesi, E. Pronsato and A. Juan are members of CONICET.

References

[1] R.A. Lemons, J. Power Sources 29 (1990) 251.
[2] H.A. Gasteiger, N. Markovic, P.N. Ross, E.J. Cairns, J. Phys. Chem. 98 (1994) 617.
[3] M. Watanabe, S. Motoo, J. Electroanal. Chem. 60 (1975) 267.
[4] H.A. Gasteiger, N.M. Markovic, P.N. Ross, J. Phys. Chem. 99 (1995) 8290.
[5] T. Massalski, Binary Alloy Phase Diagrams, vol. 2, American Society for Metals, OH, 1986, p. 1906.
[6] M.S. Löffler, H. Natter, R. Hempelmann, K. Wippermann, Electrochim. Acta 48 (2003) 304.
[7] H.A. Gasteiger, N. Markovic, P.N. Ross Jr., E. Cairns, J. Electrochem. Soc. 141 (1994) 1795.
[8] T. Frelink, W. Visscher, J.A.R. van Veen, Langmuir 12 (1996) 3702.
[9] T. Iwasita, H. Hoster, A. John-Anacker, W.F. Lin, W. Vielstich, Langmuir 16 (2000) 522.
[10] A.S. Arico, P.L. Antonucci, E. Modica, V. Baglio, H. Kim, V. Antonucci, Electrochim. Acta 47 (2002) 3723.
[11] G. te Velde, F.M. Bickelhaupt, S.J.A. van Gisbergen, C. Fonseca Guerra, E.J. Baerends, J.G. Snijders, T. Ziegler, J. Comput. Chem. 22 (2001) 931.
[12] C. Fonseca Guerra, J.G. Snijders, G. te Velde, E.J. Baerends, Theor. Chem. Acc. 99 (1998) 391.
[13] ADF2004.01, SCM, Theoretical Chemistry, Vrije Universiteit, Amsterdam, The Netherlands, http://www.scm.com.
[14] D. Becke, Phys. Rev. A 38 (1988) 3098.
[15] C. Lee, W. Yang, R.G. Parr, Phys. Rev. B 37 (1988) 785.
[16] K. Christmann, Surf. Sci. Rep. 9 (1998) 1.
[17] B.J.J. Coelman, S.T. de Zwart, A.L. Borres, B. Poelsema, L.K. Veerheij, Phys. Rev. Lett. 56 (1986) 1152.
[18] G. Papoian, J.K. Norskov, R. Hoffmann, J. Am. Chem. Soc. 122 (2000) 4129.
[19] P. Lieu, A. Logadottir, J.K. Nørskov, Electrochim. Acta 48 (2003) 3731.
[20] G.F. Cabeza, N.J. Castellani, P. Légaré, Comp. Mat. Sci. 17 (2000) 255.
[21] J.R. Kitchin, J.K. Nørskov, M.A. Barteau, J.G. Chen, J. Chem. Phys. 21 (2004) 10240, 120.